

Textual Explanations and Their Evaluations for Reinforcement Learning Policy

Ahmad Terra^{1,2}, Mohit Ahmed^{1,3}, Rafia Inam^{1,2}, Elena Fersman⁴, and Martin Törngren²

¹Ericsson Research, Ericsson AB, Stockholm, Sweden

(ahmad.terra@ericsson.com, mohit.ahmed@ericsson.com, rafia.inam@ericsson.com)

²Industrial Engineering and Management, KTH Royal Institute of Technology, Stockholm, Sweden,
(terra@kth.se, raina@kth.se, martint@kth.se)

³Faculty of Science and Technology, Uppsala University, Uppsala, Sweden,
(mohit-uddin.ahmed.2400@student.uu.se)

⁴Global AI Accelerator, Ericsson Inc., Santa Clara, CA 95054, US, (elena.fersman@ericsson.com)

Abstract—Understanding a Reinforcement Learning (RL) policy is crucial for ensuring that autonomous agents behave according to human expectations. This goal can be achieved using Explainable Reinforcement Learning (XRL) techniques. Although textual explanations are easily understood by humans, ensuring their correctness remains a challenge, and evaluations in state-of-the-art remain limited. We present a novel XRL framework for generating textual explanations, converting them into a set of transparent rules, improving their quality, and evaluating them. Expert’s knowledge can be incorporated into this framework, and an automatic predicate generator is also proposed to determine the semantic information of a state. Textual explanations are generated using a Large Language Model (LLM) and a clustering technique to identify frequent conditions. These conditions are then converted into rules to evaluate their properties, fidelity, and performance in the deployed environment. Two refinement techniques are proposed to improve the quality of explanations and reduce conflicting information. Experiments were conducted in three open-source environments to enable reproducibility, and in a telecom use case to evaluate the industrial applicability of the proposed XRL framework. This framework addresses the limitations of an existing method, Autonomous Policy Explanation, and the generated transparent rules can achieve satisfactory performance on certain tasks. This framework also enables a systematic and quantitative evaluation of textual explanations, providing valuable insights for the XRL field.

Keywords—Explainable reinforcement learning, textual explanations, rule extraction, explanation evaluation.

1 Introduction

Artificial Intelligence (AI), and especially Deep Learning (DL) algorithms, are becoming more and more adopted in industry, increasing the need for transparency and explainability given the black-box nature of DL algorithms. To address this need, Explainable Artificial Intelligence (XAI) contributes by explaining how an AI system arrives at a particular decision. As this is crucial for building user confidence and complying with AI regulations, XAI adoption is also increasing in industrial applications [1]. A subfield of XAI is XRL, which focuses mainly on understanding the RL policy (a function that maps a state to an action). Autonomous Policy Explanation (APE) [2] is an XRL method that is suitable for non-AI experts because the explanation is presented in a natural language format.

Studies suggest that textual explanations are preferred over graphical ones regardless of expertise [3], but they can also cause over-reliance on AI [4]. APE requires fixed templates that lead to rigid interactions. On the

other hand, LLMs have enabled humans to interact with machines flexibly without following a strict template. In XAI, LLMs have been used to compile attributive explanations through Retrieval-Augmented Generation (RAG) [5]. A recent study indicates that LLMs can improve XAI usability due to their narrative nature [6].

Another key to enable human trust in AI is the evaluation of explanations. In textual explanations, especially when LLMs are employed, some evaluations focus on how they are presented [6]. In a more traditional XAI setting, ground-truth explanations are rarely available. Alternatively, explanations can also be evaluated by involving humans, although this remains challenging as it is prone to bias [7].

In this article, we propose a novel framework to explain the behavior of an RL agent by generating and evaluating its textual explanations. This framework focuses on producing a list of state conditions relevant to actions with consistent categorical values. In this framework, a user can query the explanations and receive them in a natural-language format. The explanations are evaluated

on the basis of how representative they are relative to the obtained data and the given task. The main contributions are as follows:

- An implementation of an LLM to interpret queries about an RL policy.
- A method to summarize an RL policy for textual explanations. This includes techniques to define, extend, and refine predicates in the discretization of data.
- A method for extracting rules from textual explanations and evaluating them to assess their correctness.
- Two techniques to improve explanation quality.
- A framework that integrates all the above points in three different open-source environments and an industrial-telecom application.

2 Related Work

APE [2] analyzes historical data to generate explanations of conversation-like interactions between humans and an RL policy. This method can be used to generate meaningful counterfactuals and filter attributive explanations [8]. In operation, predicate functions are used to convert numerical values into textual information. It has a limitation in scaling up to large predicate sets due to the employed Quine-McCluskey algorithm [9]. The computational complexity of the algorithm increases exponentially with the predicate size. In addition, when all possible states are present in an action, there is no indication of the condition under which the RL agent would take that action. Furthermore, APE can generate duplicate explanations when similar conditions appear for different actions. Our proposed method addresses these limitations by presenting frequent conditions and suppressing duplicates with linear growth in computation relative to the predicate size.

Generating textual explanations can also be done by adding explainer modules to the Deep Neural Network (DNN) model, as done in InterpNET [10] and EPRelu-CSGNN-MALSTCAM [11]. In these works, the classifier module was initially trained, followed by training the DNN explainer module. Although a higher accuracy was achieved, it contradicted the spirit of explainability in minimizing the black-box properties of the model. A more direct method was presented in [12], where the most relevant nodes were identified and presented in a textual explanation using a predefined template. Alternatively, Poli et al. proposed a method to generate a textual explanation for semantic image annotation [13], also using a predefined template. Similar to these methods, we use a predefined template, but instead of generating a local explanation as used in the aforementioned methods, our

method combines conditions covering the global or cohort scope.

LLMs can process and generate textual information in a flexible manner with a less rigid format. An implementation of an LLM to explain an AI model was presented in [5]. In that work, RAG was used to collect relevant information about the data instances being explained, including their attribution values. More thorough frameworks have been proposed in TalkToModel [14] and CoSQL [15], where multiple XAI techniques are integrated to handle different types of explanations. They focused on the correctness of the generated parsing command for collecting data from the database and converted the results into text using an LLM. Our proposed method uses an LLM as a question interpreter, and our focus is on generating textual explanations from the parsed data.

In the XRL field, NavChat [16] used an LLM to justify and explain the decisions made by the RL agent with DeepSHAP [17] to identify impactful features. In addition, HighwayLLM [18] used an LLM to explain the RL policy and ensure safety. In the telecom field, Ameur et al. [19] used an LLM to explain the RL agent controlling a network slicing problem. Although most previous methods are applied to specific applications, ours is application-agnostic, as exemplified in several environments, including an industrial application.

In the XAI-rule-extraction field, a direct extraction of a DNN model is carried out through a Decision Tree (DT) [20]. The FRBES [21] extracts fuzzy rules from a DNN, which employs an attributive explainer to prioritize important features for constructing the rules. CGX [22] uses a decomposition method to extract rules from the hidden representation of a DNN model, where multiple objectives can be defined to fit the explainability needs. In RL, Engelhardt et al. extracted rules from trained agents using a DT [23]. Although they used rules as explanations, ours is the opposite, i.e., the explanation is converted into rules with consistent threshold values. This technique bridges textual explanations and their evaluation.

Most evaluation metrics in XAI are proposed for attributive explanations. Researchers have proposed many metrics with similar terms, but they sometimes have significantly different formulations [24]. Challenges such as inconsistent findings or oversimplification were also reported in [25]. In XAI with rule extraction, information power is proposed to evaluate the explanation involving non-expert users during the evaluation [26]. In textual explanations with LLMs, evaluations often focus on the correctness of parsing the required information [14, 15]. Our experiment and evaluation follow the suggestions of [25], which addresses real-world telecom use cases while being evaluated in a rather simplified scenario. Instead of evaluating the explanations in their local scope, we analyzed the coherence of the explanations to ensure

consistency.

3 Proposed Framework

In RL, an agent learns through interactions with an environment — an external system that provides a state that represents its condition (s), receives an action that influences it (a), and returns a reward as feedback (r). The states are typically represented by the input features with continuous values, and the predicate functions (P) can be used to discretize and represent their semantic information. In this work, it is assumed that the RL agent has learned its policy (π) and stored the replay data consisting of a set of states (S), actions (A), and rewards (R) in an SQLite database.

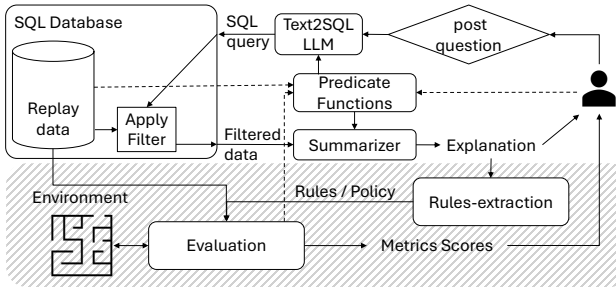


Figure 1: Overall framework of the proposed method, where the top half illustrates the explanation generation process, while the shaded area represents evaluation using rule extraction.

We propose a framework to explain an RL policy by summarizing the relationships between states and actions in a textual format. It can interactively answer questions such as “*when will you do <action>?*” or “*what will you do on <condition>?*”. A condition (c) is a set of partial or complete logical statements that construct a discrete state. The overall framework is illustrated in Fig. 1, where it begins with a user asking a question, which is then converted into a Structured Query Language (SQL) query via a text-to-SQL component to filter the data. The filtered data are then summarized using our proposed method to generate textual explanations. These explanations are then converted into rules for evaluation using replay data and the environment. The details of each stage are presented in the following subsections.

3.1 LLM as Explainer Interface

The LLM is used to interpret questions about the RL policy to convert them into an SQL query [27] to retrieve the relevant data. The user’s question is accompanied by a few-shot learning to prompt the LLM to ensure the correct SQL query format. Once generated, the query is then executed on the database, and the filtered data is passed to the summarizer. The LLM serves solely as the

interface for query interpretation, while the summarizer performs data aggregation; the two are decoupled to maintain transparency and control.

3.2 Clustering-Based Summarizer (CBS)

The result of the above step is expected to be a long list of data instances relevant to the query. Since these are numerical, we propose the Clustering-Based Summarizer (CBS) to summarize and present them in a textual format.

3.2.1 Predicate Function

Let us define p as a predicate function that takes a numerical state ($s \in S$) and returns a set of logical values or levels indicating how the state complies with p . In APE, P is a set of Boolean predicate functions that discretize the state. Let f be the feature name of a complete feature set F ($f \in F$), thus $p^f(s)$ is the predicate function for the feature f . With binary functions, the predicate can be formalized as $p^f(s) = \mathbb{I}(s^f > l^f)$ where l is a limit/threshold and \mathbb{I} is an indicator function that returns a Boolean value. Thus, each input feature is converted into a true/false or high/low value.

In this framework, an expert can manually define the predicate functions. Alternatively, statistical methods can be used, such as choosing the median or a certain quantile value of the data as a threshold. However, this can be problematic if the data distribution has high density around it because many similar instances would be discretized to different values. Therefore, we propose a technique to determine the predicate limits, as shown in Algorithm 1. Here, we slice the data by feature names (S^f) to train a DT with a maximum of n_{cat} leaf nodes. L is the set of limits obtained from the splitting values in the DT.

Algorithm 1 Gini-based Predicate Limit Generation

Require: States: S ; Actions A ; Feature names F ; Number of categories n_{cat} ;

- 1: $L \leftarrow \emptyset$
- 2: **for** $f \in F$ **do**
- 3: $X \leftarrow S^f; Y \leftarrow A$
- 4: $DT^f \leftarrow \text{train_DT}(X, Y, n_{cat})$ {Train a decision tree with maximum of n_{cat} leaf nodes}
- 5: $\Theta \leftarrow \text{get_splitting_values}(DT^f)$
- 6: $L^f \leftarrow L^f \cup \Theta$ {append threshold(s) to L^f }
- 7: **end for**
- 8: **return** L

3.2.2 Predicate Levels

When a binary function is used, each predicate function outputs two levels of information. In a binary system, categorizing a feature into “low”, “medium”, and “high”

requires three different functions and generates three digits/elements to represent them. Thus, we propose to use a categorical predicate formulation in Eq. (1) to simplify this process. In this way, different levels of the same feature can be represented using a single digit/value.

$$P_f(s) = \begin{cases} -1.0, & s^f \leq L_0^f \\ \frac{2}{n_{cat}-1} - 1, & L_0^f < s^f \leq L_1^f \\ \vdots & \\ \frac{2 \times (n_{cat}-2)}{n_{cat}-1} - 1, & L_{n_{cat}-2}^f < s^f \leq L_{n_{cat}-1}^f \\ 1.0, & L_{n_{cat}-1}^f < s^f \end{cases} \quad (1)$$

3.2.3 Clustering Summarization

We cluster the discretized data using the K-means algorithm to collect similar instances into one group and use the elbow method to determine the number of clusters. The K-means algorithm is used because the categorical values contain magnitude information for each relevant predicate. In each cluster, unique instances are computed and sorted in descending order. As a cluster may have outliers or infrequent instances, we set an inclusion threshold $\theta \in (0, 1]$ to filter these out. We collect the frequent discrete states in Q and iterate over all predicates P . Let Q^p be the set of discrete values of Q for the predicate p , ψ_v^p be the tuple of the predicate function p and the value assigned to it ($\psi_v^p = \langle p, p(s) \rangle$). When there is one unique discrete predicate value in the cluster ($|\{Q^p\}| = 1$), ψ_v^p is added to the condition c_k . After collecting the conditions from each cluster, the summary is returned as a list of conditions $\{c_0, c_1, \dots, c_k\} \in C$ as presented in Algorithm 2.

3.2.4 Textual Explanation

Converting a condition into a textual explanation follows the defined predicates. For example, p_1 , p_2 and p_3 are binary predicate functions that discretize features f_1 , f_2 , and f_3 , respectively. If the resulting vector is $c = (-1, 1, -1)$, then the textual information is " f_1 is low AND f_2 is high AND f_3 is low". When multiple conditions are identified, they are concatenated with the "OR" operator. In categorical discretization, textual levels can be extended to accommodate more values, for example, when $n_{cat} = 5$, textual levels can be defined as "Very Low", "Low", "Medium", "High", and "Very High". When multiple levels are identified for the same predicate, we compress them by combining them into a single criterion, such as "Above Low" or "Below Medium". We use a template rather than an LLM to convert a condition into a textual explanation to save computational resources, as LLMs are not designed to process numerical information. Additionally, we experimented with DeepSeek-14B, DeepSeek-32B, and Mixtral-8x7B-Instruct to convert

Algorithm 2 Clustering-based Summarization (CBS)

Require: States S ; Predicate funcs P ; Inclusion thresh θ ;

- 1: $C \leftarrow \emptyset$
- 2: $D \leftarrow P(S)$ {Discretize the filtered states}
- 3: $K \leftarrow \text{KMeans_clustering}(D)$
- 4: **for** $k \in K$ **do**
- 5: $n \leftarrow |D_k|$ {Count the number of D_k }
- 6: $U_k \leftarrow \text{count_unique}(D_k)$ {Collect frequency of D_k }
- 7: $U_k^\downarrow \leftarrow \text{sort}(U_k)$ {Sort in descending order}
- 8: **for** $i = 1, \dots, |U_k^\downarrow|$ **do**
- 9: $M[i] \leftarrow \sum_{j=1}^i U_k^\downarrow[j]$ {cumulative sum}
- 10: **if** $M[i] \geq \text{int}(\theta \times n)$ **then**
- 11: $m \leftarrow i$ {last index within threshold}
- 12: **break**
- 13: **end if**
- 14: **end for**
- 15: $Q \leftarrow \{U_k^\downarrow[1], \dots, U_k^\downarrow[m]\}$ {keep top-n U_k^\downarrow }
- 16: $c_k \leftarrow \emptyset$
- 17: **for** $p \in P$ **do**
- 18: **if** $|\{Q^p\}| = 1$ **then**
- 19: $c_k \leftarrow c_k \cup \langle p, Q_0^p \rangle$ {append ψ_p^Q to c_k }
- 20: **end if**
- 21: **end for**
- 22: $C \leftarrow C \cup c_k$ {append c_k to C }
- 23: **end for**
- 24: **return** C

the filtered data into text, but they discarded a fraction of the information and had flaws in presenting the observations.

3.3 Rules Extraction

As textual explanations imply a correlation between conditions and actions, humans may assume that when a condition is met, the same action will follow. We propose a method for converting textual explanations into rules, presented in Algorithm 3. The first step in this process is to collect the conditions for each action. However, the same condition may lead to different actions due to the discretization process. Thus, further information is needed to convert textual explanations into rules in which the occurrence (o) of a condition can be used to determine an action. For example, if action a is taken more frequently than the others under the same conditions, then the generated rules will select this action.

The second step is to assign a weight that indicates the occurrence of every condition in all actions. This is achieved by computing the state occurrence from the replay data. Let us define the total number of instances as N_{total} , the number of instances in a condition as N_c , the number of instances in an action as N_a , and the number

Algorithm 3 Rules Extraction from Explanations

Require: States: S ; Actions: A ; Predicate functions P ;
 Weight function w ; Inclusion threshold θ ;

- 1: $\mathcal{R} \leftarrow \emptyset$
- 2: **for** $a \in \text{unique}(A)$ **do**
- 3: $S_a \leftarrow \{s \in S \mid \pi(s) = a\}$
- 4: $C_a \leftarrow \text{Summarize}(S_a, P, \theta)$ {Algorithm 2 or APE}
- 5: $\mathcal{R}_a \leftarrow \emptyset$
- 6: **for** $c_a \in C_a$ **do**
- 7: $o_{c,a} \leftarrow w(S, A, c_a, a)$
- 8: $\mathcal{R}_a \leftarrow \mathcal{R}_a \cup \langle c_a, o_{c,a} \rangle$
- 9: **end for**
- 10: $\mathcal{R} \leftarrow \mathcal{R} \cup \mathcal{R}_a$
- 11: **end for**
- 12: **return** \mathcal{R}

of instances in a condition with the same action as N_{ca} . We then examine the following formulas to determine the best weighting function (w) to select the action: $w_1 = \frac{N_{ca}}{N_a}$, $w_2 = \frac{N_{ca}}{N_c}$, $w_3 = \frac{N_{ca}}{N_{total}}$, and $w_4 = \frac{N_{ca}}{N_a} \times \frac{N_{ca}}{N_{total}}$. The percentage of conditions that appear over all data with the same action is indicated by w_1 , while w_2 is the percentage of an action taken under the same condition. w_3 computes the percentage of the same condition-action over all data and w_4 is the combination of w_1 and w_3 .

Finally, each condition (c_a) is coupled with its occurrence ($o_{c,a}$) to construct a rule for action a ($\mathcal{R}_{c,a}(s) = \mathbb{I}(P(s) = c_a).o_{c,a}$). In other words, this can be interpreted as "when condition c_a is met, action a is taken with $o_{c,a}$ occurrences". To utilize the generated rules \mathcal{R} , we use the following formula in Eq. (2) to select the best action (a^*), where C_a is the set of conditions for an action:

$$a^* = \arg \max_{a \in A} \sum_{c \in C_a} \mathcal{R}_{c,a}(s) \quad (2)$$

In the generated rules, a state may not be covered in any action due to the removal of infrequent occurrences or new conditions that have not been observed in the replay data. To solve this, we propose an approximation function (Algorithm 4) to cover a state that is not present in any condition/rule and determine its action. Euclidean distance is used as the data are in a normalized range. Using this approach, similar textual explanations, including APE explanations, can be converted into rules. If the evaluation results are satisfactory, the black-box agent can be replaced by these transparent rules.

3.4 Explanation Evaluation

Textual explanations contain information that is easily understood by humans. The length of an explanation plays an important role in understanding it. Formally, the length of the explanation is defined by the number

Algorithm 4 State-Condition Approximation

Require: state s ; Conditions C ; Predicates P ; Features F

- 1: $d_{min} \leftarrow \infty$
- 2: **for** $c \in C$ **do**
- 3: $m_c \leftarrow \text{median}(c, P)$ {bin centers of c given P }
- 4: $d \leftarrow \sqrt{\sum_{f \in F} (m_f - s_f)^2}$ {Euclidean distance}
- 5: **if** $d < d_{min}$ **then**
- 6: $d_{min}, c_{min} \leftarrow d, c$
- 7: **end if**
- 8: **end for**
- 9: **return** c_{min}

of conditions generated ($E_{len} = |C|$). Although longer explanations may exhaust one's mental capacity, they capture more detailed information than the shorter ones.

As mentioned in Section 3.3, the same condition may appear in multiple actions. As this may lead to ambiguity, we count the number of duplicated conditions as part of our evaluation ($E_{duplicate} = |\{C_i \mid \exists a_1 \neq a_2, C_i \in C^{a_1} \wedge C_i \in C^{a_2}\}|$). These two metrics are categorized as explanation properties, as they directly assess the explanations without comparing them with the underlying replay data used to generate them.

Furthermore, we use the replay data for evaluation, where we count the states that cannot be mapped to any condition on any action, ($E_{approx} = \frac{1}{|S|} \sum_{s \in S} \mathbb{1}(\forall a, P(s) \notin C^a)$). This metric can be considered a coverage metric that shows how many states are not covered by the generated explanations/rules.

The states in the replay data are then used to infer the actions of the proposed rule extraction. In this case, the actions in the replay data can be considered as the ground truth of the policy being explained. Consequently, we can determine the fidelity of the explanations by comparing them using supervised learning metrics such as accuracy (E_{acc}), recall (E_{rec}), and F1 (E_{F1}).

In RL, the reward is an indicator of how an agent performs in the environment. Since the aim of this work is to explain the RL agent's behavior, we can also evaluate the performance of the explanation by converting it using the proposed rule extraction method. This is done by deploying the rules in the same environment in which the RL agent was previously trained. We collect three metrics in doing so, which are: cumulative reward in an episode ($E_{CR} = \sum_{t=0}^T r_t$), total time steps in an episode ($E_{TS} = T$), and average reward per time step ($E_{AR} = \frac{E_{CR}}{E_{TS}}$), where r is the reward and T is the total time steps. Note that the reward is a quantitative measure that can be replaced by any other numerical indicator, such as cost savings, Key Performance Indicator (KPI), energy consumption/savings, etc. Thus, the proposed evaluation method can be used to indicate the cost/compromise if

one chooses to use the extracted transparent agent. This performance evaluation enables better trade-off analysis between black-box and transparent agents.

3.5 Predicate Refinement

In Section 3.2.1, we presented a method for defining the predicate thresholds based on the Gini score of the filtered data. It initializes the predicates based only on the data, neither considering the generated explanations nor the rules. In this subsection, we introduce methods for refining the predicate definitions by considering the generated rules. We propose a technique to reduce $E_{\text{duplicate}}$ with coherent and less conflicting information among actions. Alternatively, we also propose a technique to improve the fidelity (F1) of the explanations.

Algorithm 5 Minimize Duplicated Conditions Among Actions

Require: States: S ; Actions A ; F1 score $f1$; Number of categories n_{cat} ; Duplicated Conditions C ; Predicate Limits L ; Max Recommendations m ; Iteration Budget b ;

- 1: $L_{\text{update}} \leftarrow L; L_{\text{init}} \leftarrow L; i \leftarrow 0$
- 2: $L_c \leftarrow \emptyset$ {collection of proposed limits}
- 3: $D \leftarrow \emptyset$ {tracking count of duplicate}
- 4: **while** $i < b$ **do**
- 5: $F \leftarrow \emptyset$ {tracking F1 score}
- 6: **for** $c \in C$ **do**
- 7: $S_c, A_c \leftarrow \text{filter}(S, A, c)$ {filter data that satisfy c }
- 8: $DT_f \leftarrow \text{train_DT}(S_c, A_c, n_{\text{cat}})$ {Train a decision tree with maximum of n_{cat} leaf nodes}
- 9: $\Theta \leftarrow \text{get_thresholds}(DT_f)$
- 10: $\Theta^\uparrow \leftarrow \text{sort}(\Theta)$ {sort from root to the farthest leaf}
- 11: **for** $\theta \in \Theta^\uparrow$ **do**
- 12: $j \leftarrow \text{argmin}(\text{abs}(L_{\text{update}}^f - \theta^f))$ {nearest limit}
- 13: $L_{\text{update}}^{f,j} \leftarrow \theta^f$
- 14: $d, f1 \leftarrow P.\text{apply}(L_{\text{update}})$ {get duplicate & f1}
- 15: $D \leftarrow D \cup d; L_c \leftarrow L_c \cup L_{\text{update}}; F \leftarrow F \cup f1$
- 16: $L_{\text{update}} \leftarrow L_{\text{init}}$
- 17: **end for**
- 18: **if** $\max(F) > f1$ **then**
- 19: $L_{\text{init}} \leftarrow L_{\max(F)}; f1 \leftarrow \max(F)$
- 20: **end if**
- 21: **end for**
- 22: $i \leftarrow i + 1$
- 23: **end while**
- 24: $k \leftarrow \text{argmin}(D)$
- 25: **return** $L_{\text{candidate},k}$

The technique for minimizing duplicate conditions

($E_{\text{duplicate}}$) is presented in Algorithm 5. It iterates over the duplicated conditions (line 7) and then builds a DT model from the filtered data to obtain new threshold values (Θ). Each value is then evaluated using the duplicates and F1 score. If the proposed change increases the F1 score, then the updated threshold is used in the next iteration. The updated thresholds are collected during these iterations, and the one with the lowest duplicates is returned.

Algorithm 6 Maximize F1 Score

Require: States: S ; Feature Names F ; Predicate Limits L ; Adjustment rate α ; Iteration Budget b ;

- 1: $f1 \leftarrow P.\text{apply}(L)$
- 2: $f1_1 \leftarrow f1; f1_2 \leftarrow f1$
- 3: **for** $f \in F$ **do**
- 4: **for** $i \in L^f$ **do**
- 5: $X \leftarrow S^f$ {collect feature f values}
- 6: **if** $\text{len}(L^f) > 1$ **then**
- 7: $X \leftarrow \{s_f \in S_f | L_{i-1}^f \leq s_f < L_{i+1}^f\}$
- 8: **end if**
- 9: $\theta \leftarrow L_i^f; t \leftarrow \text{False}; j \leftarrow 0$
- 10: **while** (t)AND($j < b$) **do**
- 11: $k \leftarrow 1$
- 12: **while** ($f1_1 == f1$)AND($k < b$) **do**
- 13: $\theta_1 \leftarrow \theta - k \times \alpha \times (\theta - \min(X))$
- 14: $f1_1 \leftarrow P.\text{apply}(\theta_1); k \leftarrow k + 1$
- 15: **end while**
- 16: $k \leftarrow 1$
- 17: **while** ($f1_2 == f1$)AND($k < b$) **do**
- 18: $\theta_2 \leftarrow \theta + k \times \alpha \times (\max(X) - \theta)$
- 19: $f1_2 \leftarrow P.\text{apply}(\theta_2); k \leftarrow k + 1$
- 20: **end while**
- 21: $m \leftarrow \text{argmax}(\{f1, f1_1, f1_2\})$
- 22: **if** $m == 0$ **then**
- 23: $t \leftarrow \text{True}$
- 24: **end if**
- 25: $L^{f,i} \leftarrow \theta_m; f1 \leftarrow f1_m$
- 26: $j \leftarrow j + 1$
- 27: **end while**
- 28: **end for**
- 29: **end for**
- 30: **return** L

The technique for maximizing the F1 score is proposed in Algorithm 6, in which the predicate thresholds are adjusted around their original values. It starts by computing the F1 score of the current setup (L) and then iterates over all features F and each threshold within it (L^f). If the predicate function is nonbinary (level ≥ 2), it collects the data that will be affected by the threshold ($L^{f,i}$; line 7). For these selected data, we then try to decrease (line 13) or increase (line 18) the threshold and collect the F1 scores. The threshold with the highest F1 value is then used in the next iteration (lines 21-25).

4 Experiments and Evaluations

In this section, we first present the experimental setup. We then present the results of the comparison of APE and CBS, followed by experiments with varying parameters in CBS.

4.1 Experiment Setup

In this work, we used three open-source environments from the Gymnasium¹ library: LunarLander-v2, MountainCar-v0, and CartPole-v1. We used pre-trained Deep Q-Network (DQN) agents² for these environments to ensure the optimal performance of the agent and enable reproducibility.

Additionally, we also experimented with an industrial use case of a proprietary Remote Electrical Tilt (RET) simulated environment, where the goal is to optimize its KPIs by controlling the tilt of the base-station antennas. 10,000 User Equipments (UEs) are uniformly distributed across the environment, and seven Base Stations (BSs) are configured in a hexagonal shape, as shown in Fig. 2. The state comprises UEs interference, Signal-to-Interference-plus-Noise-Ratio (SINR), Reference-Signal-Received-Power (RSRP), throughput, and antenna tilt angle. The actions are discrete: 1° up-tilt, no tilt, and 1° down-tilt. The reward is formulated as $R = 0.6 \times \mathbb{I}(\text{RSRP} > -110\text{dBm}) + 0.4 \times \mathbb{I}(\text{SINR} > 13\text{dB})$. The first part of the reward indicates the coverage of the signal, whereas the latter indicates the quality. Each antenna is controlled by an independent RL agent that is trained using a DQN with reward decomposition (DQNRD) [28] sharing the same policy.

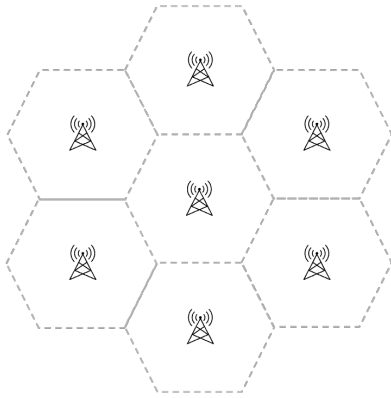


Figure 2: Layout of base stations used in RET use case.

For the explainer interface, the DeepSeek-R1-Distill-Llama-70B model [29] with a temperature of 0.5 is used. The replay data was collected by running the trained agents in their environments until they reached 10,000 time steps and completed the final episodes. It starts

with a seed equal to 0 and increases by 1 in every episode. This data is then used to generate explanations, extract rules, and evaluate them. For performance evaluation, we ran ten episodes for every set of experiments with the same seed numbers (0 to 9). This seed number was kept identical for all parameter configurations to allow for a valid comparison. The performance of RET is only available in Section 4.7 because it took significant resources to run a single simulation.

4.2 Sample of the Explanations

The proposed framework was built to summarize the observed data and present them in a textual format. A sample of the generated explanations in this experiment is shown in Fig. 3, in which we show only a partial explanation of the RET use case to save space. Other types of questions, such as "What will you do when RSRP is low?" can also be asked to generate explanations in a similar format.

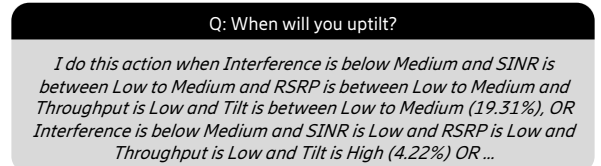


Figure 3: Partially generated textual explanations.

4.3 APE vs CBS

In this subsection, we compare the evaluation of APE with our proposed method, CBS. We varied the weighting functions (w) and the predicate definitions for both methods. The inclusion thresholds were varied only for CBS because APE always includes the entire data ($\theta = 1.0$). The maximum number of clusters (k) in CBS was set to 40. In this experiment, we used only two levels of predicates (Low and High) due to APE's limitation on binary predicates. The predicate functions for both methods were kept the same. The mean values of the metrics for each setup in this comparison are shown in Table 1. Additionally, the values of reward-related scores (E_{CR} and E_{TS}) are normalized by the highest value in each environment ($\text{Norm}(x) = x/\max(\text{abs}(X_{\text{env}})) \times 100\%$) to fit the table width and ensure a fair averaging.

In the LunarLander and RET environments, there is no approximated state to decide the action ($E_{app} = 0.0$) on APE explanations, i.e., the generated rules cover any possible state. This is because the Quine-McCluskey algorithm is used to minimize the binary representation in a complete manner without discarding any binary state. However, APE did not generate any explanation for the CartPole and MountainCar environments ('-'). All possible combinations of discrete states appeared in

¹<https://gymnasium.farama.org>

²<https://github.com/DLR-RM/rl-trained-agents/>

Table 1: Evaluation of APE (A) and CBS (C) in different environments.

Env	CartPole		LunarLander		MountainCar		RET	
	A	C	A	C	A	C	A	C
E_{app}	-	1.7	0.0	17.2	-	1.5	0.0	3.1
E_{len}	-	13.6	56.9	24.4	-	7.6	16.8	17.9
E_{dup}	-	3.8	1.9	2.3	-	2.6	0.0	3.7
E_{acc}	-	73.2	42.8	41.4	-	75.1	72.0	72.6
E_{rec}	-	73.2	45.5	36.4	-	59.6	62.4	57.3
E_{F1}	-	72.3	35.1	28.9	-	54.0	60.2	52.4
E_{CR}	-	17.4	-69.2	-35.2	-	-83.3	-	-
E_{TS}	-	17.4	38.5	28.3	-	83.3	-	-
E_{AR}	-	1.0	-1.8	-1.2	-	-1.0	-	-

one or more action(s) in the replay data. Therefore, no rule or evaluation metric could be generated.

The explanation length of APE is significantly greater than CBS for LunarLander, whereas it is slightly smaller for RET. The duplicated conditions are also higher in the CBS than in the APE for both environments. Note that in LunarLander, APE explanations also suffer from the duplicate issue, where the same condition appears in multiple actions because the Quine-McCluskey algorithm is applied separately to each action. In terms of fidelity metrics other than accuracy in RET, APE has higher results than CBS. Performance-wise, our method has higher total (E_{CR}) and average (E_{AR}) rewards than APE on LunarLander.

4.4 Varying Parameters

Changing the predicate definition may generate conflicts with experts' knowledge. For example, an expert defines that a high SINR value is above 13 dB, but there are many data points around this value in multiple actions. Thus, shifting the threshold to 10 dB, at which the data points are separable, may lead to different results. Table 2 compares the evaluation results for the predicate thresholds defined by the Gini(G; Algorithm 1) and the median(M) for the CBS method.

Table 2: Evaluation of Median (M) and Gini (G) predicate initiators using CBS in different environments.

Env	CartPole		LunarLander		MountainCar		RET	
	G	M	G	M	G	M	G	M
E_{app}	2.1	1.2	6.8	27.6	0.0	3.0	2.2	3.9
E_{len}	11.0	16.1	24.4	24.5	7.9	7.3	16.0	19.7
E_{dup}	2.7	5.0	2.9	1.8	2.7	2.4	3.2	4.1
E_{acc}	74.0	72.4	49.0	33.8	81.8	68.3	78.2	67.1
E_{rec}	74.0	72.4	40.3	32.5	63.9	55.3	60.1	54.6
E_{F1}	72.7	72.0	35.5	22.3	59.9	48.0	55.8	49.0
E_{CR}	14.7	20.1	-35.3	-35.1	-76.8	-89.7	-	-
E_{TS}	14.7	20.1	29.2	27.3	76.8	89.7	-	-
E_{AR}	1.0	1.0	-1.2	-1.3	-1.0	-1.0	-	-

The explanations using the Gini-based predicate definition have fewer approximated states (E_{app}) than the

median, except for CartPole, indicating a better coverage of the explanations. In length (E_{len}) and duplicated conditions (E_{dup}), the results are inconclusive, where there are lower and higher scores in different environments. The predicates defined using Gini purity have higher fidelity scores than the median, showing a better representation of the summarized data. In performance metrics, the proposed Gini-based predicates have higher E_{CR} scores in MountainCar.

Table 3: Evaluation of different weighting (w) functions.

$w_{<version>}$	1	2	3	4
E_{app}	5.7	5.7	5.7	6.4
E_{len}	15.9	15.9	15.9	15.9
E_{dup}	3.1	3.1	3.1	3.1
E_{acc}	60.3	68.3	66.8	66.8
E_{rec}	57.9	57.5	54.6	56.4
E_{F1}	51.2	53.6	50.6	52.2
E_{CR}	-37.8	-31.6	-32.9	-32.4
E_{TS}	46.9	43.6	40.6	40.8
E_{AR}	-0.8	-0.7	-0.8	-0.8

Another parameter that we varied was the weighting function for rule extraction, where we aggregated the scores from all environments because four functions were checked. Table 3 shows the results, where all functions have similar E_{app} , E_{len} , and E_{dup} except that w_4 has the highest E_{app} . w_2 has the highest accuracy, F1, and reward-related (E_{CR} and E_{AR}) scores. This is reasonable because w_2 captures the percentage of relevant actions under the same condition. Therefore, w_2 was selected for subsequent experiments.

Table 4: Evaluation of different inclusion thresholds (θ).

θ	0.10	0.30	0.50	0.70	0.80	0.90	1.00
E_{app}	14.2	11.7	8.1	3.7	2.1	1.2	0.0
E_{len}	15.9	15.9	15.9	15.9	15.9	15.9	15.9
E_{dup}	4.4	4.0	3.5	3.1	3.0	2.3	1.5
E_{acc}	64.6	64.7	64.6	67.4	67.2	67.3	63.1
E_{rec}	57.9	58.0	57.6	58.5	58.1	57.8	48.4
E_{F1}	53.3	53.6	53.0	54.4	53.7	52.7	42.6
E_{CR}	-29.8	-32.8	-34.1	-33.2	-34.3	-34.7	-37.0
E_{TS}	42.3	43.5	43.7	42.3	41.3	41.7	46.1
E_{AR}	-0.7	-0.8	-0.8	-0.8	-0.8	-0.8	-0.8

The inclusion threshold (θ) is set to determine the number of instances to be included in every cluster that have been ordered by their occurrences. The lower θ , the fewer instances are included to be summarized. Table 4 presents the results of varying θ from 10% to full inclusion (100%). Although the length of the explanation (E_{len}) is not affected by the threshold, the number of approximated states (E_{app}) and duplicated conditions (E_{dup}) decrease as θ increases. This indicates that the coverage of the rules increases as more instances are included.

In fidelity metrics, the highest scores were obtained at $\theta = 70\%$, which was selected for later experiments in the following subsections. A significant drop in the fidelity scores is observed for full inclusion, indicating that infrequent instances are most likely to be outliers. Thus, the strategy of considering frequent instances is justified to achieve higher fidelity scores.

4.5 Varying Categories Levels

After varying the parameters above, we selected the following configuration for CBS based on the fidelity metrics to continue with the rest of the experiments: Gini-based predicate definition, weighting function w_2 , and $\theta = 70\%$. In this subsection, we vary the number of levels that a predicate can have from two to seven. The aggregated results for all environments are presented in Table 5. As the number of levels increases, the length of the explanations (E_{len}) increases until $n_{cat} = 6$. In contrast, the number of duplicated conditions (E_{dup}) decreases, indicating less conflicting information among the different actions. The highest fidelity scores were achieved at n_{cat} equal to 5 and 6. Although $n_{cat} = 7$ has the highest level-granularity, it has smaller explanations (E_{len}) than $n_{cat} = 6$, leading to higher uncovered conditions (E_{app}) and lower fidelity scores.

Table 5: Evaluation of different levels in all environments.

Levels	2	3	4	5	6	7
E_{app}	2.1	4.0	5.6	5.0	5.5	6.7
E_{len}	14.8	15.7	17.6	20.3	21.3	20.6
E_{dup}	2.9	1.3	1.2	0.8	0.6	0.3
E_{acc}	74.7	78.5	76.8	80.2	79.8	79.4
E_{rec}	62.0	70.3	70.3	77.6	77.7	76.4
E_{F1}	59.1	70.4	69.9	75.1	75.1	74.3
E_{CR}	-39.1	-36.6	-29.0	-32.5	-34.7	-36.7
E_{TS}	41.6	39.5	46.6	40.0	44.1	44.8
E_{AR}	-0.9	-0.9	-0.6	-0.8	-0.8	-0.8

Table 6: Evaluation of different levels in MountainCar.

Levels	2	3	4	5	6	7
E_{app}	0.0	0.0	4.5	6.3	6.3	9.0
E_{len}	7.9	12.0	13.9	15.7	21.1	19.0
E_{dup}	2.8	3.5	3.0	1.9	2.0	1.0
E_{acc}	87.9	90.0	88.2	91.6	90.5	89.0
E_{rec}	62.7	73.7	72.7	91.6	91.1	87.8
E_{F1}	60.9	77.5	76.4	86.9	86.2	84.5
E_{CR}	-69.7	-69.9	-69.8	-68.8	-81.7	-87.5
E_{TS}	69.7	69.9	69.8	68.8	81.7	87.5
E_{AR}	-1.0	-1.0	-1.0	-1.0	-1.0	-1.0

In performance evaluation, we see higher values of cumulative reward (E_{CR}) for 4, 5 and 6 levels. To analyze

the impact of more levels/categories, the results for the MountainCar environment are presented in Table 6. The cumulative rewards (E_{CR}) are significantly higher for $n_{cat} < 6$. This indicates that the extracted rules could complete the task in certain episodes ($E_{CR} = -100$ indicates failure). With this performance evaluation, the trustworthiness of the explanations is improved because it can be proven that following the explanations can lead to a completed task. Furthermore, if the extracted rules are used to replace the black-box agent, humans can analyze them, and any unwanted condition-action can be corrected or avoided.

4.6 Varying Refinement Techniques

In this subsection, we compare the different refinement techniques proposed in Section 3. Similar to Section 4.5, we compared the refinement techniques in all environments and MountainCar, and the results are presented in Table 7. The baseline for all environments uses the same parameters as in Section 4.5 with $n_{cat} = 6$ because it achieves the highest F1 and recall, while for MountainCar, we set $n_{cat} = 5$ because it has the highest cumulative rewards. We aim to analyze whether the proposed refinement techniques can further improve the results. We used a maximum recommendation (m) of 5, an iteration budget (b) of 5 to minimize duplicates, and 10 to maximize F1 with an adjustment rate (α) of 0.5.

Table 7: Evaluation of different refinement techniques for two different setups.

Levels	All Environments - 6 levels			MountainCar - 5 levels			
	Refine	base	min_{du}	max_{F1}	base	min_{du}	max_{F1}
E_{app}	5.46	5.22		4.50	6.34	3.63	1.99
E_{len}	21.32	20.62		22.30	15.70	15.60	18.70
E_{dup}	0.60	0.35		0.80	1.90	0.90	3.50
E_{acc}	79.75	79.90		80.88	91.56	92.76	93.66
E_{rec}	77.67	77.15		78.51	91.63	91.36	92.41
E_{F1}	75.09	75.09		76.18	86.95	87.68	88.90
E_{CR}	-31.70	-35.56		-30.69	-68.75	-63.20	-63.40
E_{TS}	57.86	58.34		54.44	68.75	63.20	63.40
E_{AR}	-0.55	-0.61		-0.56	-1.00	-1.00	-1.00

In both setups, the minimize-duplicate technique (min_{du}) successfully reduced the duplicated conditions (E_{dup}). It also reduced the length of the explanation (E_{len}) and the approximated states (E_{app}). This refinement technique also improved E_{acc} in both setups. Although E_{CR} in MountainCar is improved, the aggregated results from all environments have lower scores.

On the other hand, the maximize-F1 technique (max_{F1}) increases the length of the explanation (E_{len}) in both setups. As reducing E_{dup} is not the focus of this technique, this score increased in both setups. The goal of improving the F1 score was achieved, as shown by the improvement in all fidelity scores. Interestingly, cumulative reward scores (E_{CR}) are also improved, and

in MountainCar the score could be further improved by more than five points.

4.7 RET Results

For the RET environment, we selected a few configurations, as shown in Table 8, along with the black-box agent (DQNRD). With six levels of categories, the explanations from CBS achieve a higher fidelity than those from APE. To obtain a representative explanation of the RET agent, six levels of categories should be used because they have high fidelity scores. Performance-wise, they are all relatively similar and show slightly compromised performance (E_{AR}), considering that the maximum value is 1 (10 when multiplied). If we want to replace the black-box agent with a transparent one, CBS with binary categories has the least compromised performance. Furthermore, by showing the reward components, we observe that RSRP is improved in this setup. In this way, the operator can anticipate the cost/gain of different factors when replacing the black-box agent with a transparent one.

Table 8: Evaluation of the RET environment.

Method	APE	CBS		DQNRD
Initiator; Levels	M;2	M;2	G;6	-
θ	1.0	0.7	0.7	-
Refinement	none	min_{du}	max_{F1}	none
E_{app}	0.00	2.30	2.86	2.95
E_{len}	17.00	16.80	20.00	21.40
E_{dup}	0.00	2.30	0.00	0.00
E_{acc}	72.02	70.43	80.17	78.86
E_{rec}	62.41	63.40	72.93	72.15
E_{F1}	60.17	59.34	70.74	69.50
E_{CR}	10.54	10.88	10.10	9.94
E_{TS}	20	20	20	20
$E_{AR} (\times 10)$	5.27	5.44	5.05	4.97
E_{AR} (RSRP $\times 10$)	2.85	2.93	2.82	2.79
E_{AR} (SINR $\times 10$)	2.42	2.51	2.23	2.18
				2.65

5 Discussion

In this work, we demonstrated that LLMs are suitable for interpreting questions to trigger summarization. We did not use an LLM to perform data summarization because LLMs are designed to process textual information rather than numerical data. In the agentic AI era, the proposed framework has the potential to become a building block for explainer agents. This saves resources by not feeding lengthy numerical data to a highly complex LLM, thereby avoiding its computationally intensive inference step.

When all conditions appear in one queried action, APE cannot generate any informative explanation. Our CBS method addresses this by focusing on frequent states to always generate explanations successfully. We also showed that categorical predicates (not binary) improved the

quality of explanations. APE utilizes Quine-McCluskey with a computational complexity of $\frac{3^{|P|}}{|P|}$ that grows with the number of predicates ($|P|$). On the other hand, CBS uses the clustering method with complexity $O(|S| \times |P| \times k^2 \times i)$, where $|S|$ is the size of the data, i is the iteration, and k is the size of the cluster. Thus, APE can grow exponentially with respect to the discretization granularity, whereas CBS grows linearly. Furthermore, our method can compress the explanation by combining multiple predicate values into a single statement.

Our proposed explanation-to-rules conversion can be used to evaluate the correctness and potentially replace the black-box agent when performance trade-offs are acceptable. By deploying the rules in the environment, they are evaluated to determine whether performance remains high or is compromised. Due to the Markovian nature of RL’s formulation, a few mistakes can significantly affect the final outcome. This occurred for the rules in the Cart-Pole and LunarLander environments, where the correct actions should have been taken in certain critical states. Additionally, the explanations/rules imitated the historical data (not directly learned in the environment) with limited expressivity. On the other hand, the extracted rules in the MountainCar environment could complete the task. It shows that the extracted rules can replace the black-box agent to perform the task. Similarly, in the RET environment, replacing the black-box agent with the extracted rules slightly compromised performance. Furthermore, the evaluation scores in these two environments can be improved using the proposed refinement techniques. This shows that transparent rules with satisfactory performance can be extracted using CBS, whereas a more complex model (e.g., deep RL) is still required for more complex tasks.

The proposed rule extraction method enables fidelity evaluation of textual explanations. These metrics are important for evaluating the explanation quality for retrospective analysis because they do not affect the decision-making process. We have shown through the experiments how the parameters affected and improved the fidelity scores. The improvement in the fidelity score is crucial for understanding complex model behavior, as some of them cannot be replaced by transparent ones. Furthermore, the coherence of the explanations was indicated by duplicate conditions, which were minimized through a refinement technique.

6 Conclusion and Future Work

In this article, we have presented a framework for explaining a trained RL policy using historical data by generating textual explanations, extracting rules, and evaluating their properties, fidelity, and performance. This framework can support real-time operator/expert decision-making (e.g., retrospective analysis of an agent’s

tilt recommendation before execution). Their knowledge can be incorporated into predicate definitions, and automatic generation has also been proposed as an alternative. The evaluation procedure provides systematic measures of textual RL explanation quality. We have shown that the proposed CBS addresses the issues in APE with comparable performance. Predicate generation based on the Gini value has better fidelity than statistical quantiles. In addition, the proposed refinement techniques could further improve the explanation quality. With the proposed method, the black-box model can be replaced with a transparent one if the performance loss is tolerable.

This work can be extended to find anomalies by inverting the rules in the clustering. The framework can also be used for supervised learning problems, where performance evaluation is no longer relevant, but fidelity evaluation can be performed directly with ground truth labels. Although extending this work with attributional explanations is direct, integrating other types of explanation, such as contrastive or counterfactual, requires further investigation. Alternatively, a potential extension is to incorporate non-tabular states, such as visual inputs, via concept-embedding techniques. Another possible future direction is to investigate the adaptability of the transparent agent to continue learning, resembling the RL agent on deployment.

Acknowledgement

This work was partially supported by the Wallenberg AI, Autonomous Systems and Software Program (WASP) funded by the Knut and Alice Wallenberg Foundation and the TECoSA Centre for Trustworthy Edge Computing Systems and Applications. The authors thank Agustín Valencia and Alexandros Nikou for providing valuable feedback that helped improve the clarity of the paper.

References

- [1] I. Ahmed, G. Jeon, and F. Piccialli, “From artificial intelligence to explainable artificial intelligence in industry 4.0: A survey on what, how, and where,” *IEEE Transactions on Industrial Informatics*, vol. 18, no. 8, pp. 5031–5042, 2022.
- [2] B. Hayes and J. A. Shah, “Improving Robot Controller Transparency Through Autonomous Policy Explanation,” in *Proceedings of the 2017 ACM/IEEE International Conference on Human-Robot Interaction*. Vienna Austria: ACM, Mar. 2017, pp. 303–312.
- [3] L. Malandri, F. Mercurio, M. Mezzanzanica, and N. Nobani, “ConvXAI: a System for Multimodal Interaction with Any Black-box Ex- plainer,” *Cognitive Computation*, vol. 15, no. 2, pp. 613–644, Mar. 2023. [Online]. Available: <https://doi.org/10.1007/s12559-022-10067-7>
- [4] G. He, N. Aishwarya, and U. Gadiraju, “Is conversational xai all you need? human-ai decision making with a conversational xai assistant,” in *Proceedings of the 30th International Conference on Intelligent User Interfaces*, ser. IUI ’25. New York, NY, USA: Association for Computing Machinery, 2025, p. 907–924. [Online]. Available: <https://doi.org/10.1145/3708359.3712133>
- [5] S. Tekkesinoglu and L. Kunze, “From feature importance to natural language explanations using llms with rag,” in *MAI-XAI@ECAI*, 2024. [Online]. Available: <https://ceur-ws.org/Vol-3803/paper8.pdf>
- [6] A. Zytek, S. Pidò, and K. Veeramachaneni, “LLMs for XAI: Future Directions for Explaining Explanations,” in *Proceedings of the 2024 ACM CHI Workshop on Human-Centered Explainable AI (HCXAI)*, Honolulu, HI, USA, May 2024, presented at HCXAI workshop, in conjunction with ACM CHI 2024.
- [7] M. A. Kadir, A. Mosavi, and D. Sonntag, “Evaluation Metrics for XAI: A Review, Taxonomy, and Practical Applications,” in *2023 IEEE 27th International Conference on Intelligent Engineering Systems (INES)*, Jul. 2023, pp. 000111–000124, iSSN: 1543-9259. [Online]. Available: <https://ieeexplore.ieee.org/document/10297629/>
- [8] M. Hefny, A. Terra, and A. Valencia, “Comprehensive reinforcement learning explanations using queries,” in *Explainable Artificial Intelligence*, R. Guidotti, U. Schmid, and L. Longo, Eds. Cham: Springer Nature Switzerland, 2025, pp. 27–40.
- [9] E. J. McCluskey, “Minimization of boolean functions,” *The Bell System Technical Journal*, vol. 35, no. 6, pp. 1417–1444, 1956.
- [10] S. Barratt, “Interpnet: Neural introspection for interpretable deep learning,” in *Proceedings of NIPS 2017 Symposium on Interpretable Machine Learning*, Long Beach, CA, USA, 2017, p. 47–53.
- [11] B. P. Sheela, H. Girisha, and B. Sreepathi, “An Efficient EPReLU-CSGNN-MALSTCAM and SSOA-Based Explainable Artificial Intelligence (XAI) to Generate Textual Explanations,” *SN Computer Science*, vol. 6, no. 6, p. 594, Jun. 2025. [Online]. Available: <https://doi.org/10.1007/s42979-025-04115-w>
- [12] I. García-Magariño, R. Muttukrishnan, and J. Lloret, “Human-centric ai for trustworthy iot systems with

explainable multilayer perceptrons,” *IEEE Access*, vol. 7, pp. 125 562–125 574, 2019.

[13] J.-P. Poli, W. Ouerdane, and R. Pierrard, “Generation of textual explanations in xai: the case of semantic annotation,” in *2021 IEEE International Conference on Fuzzy Systems (FUZZ-IEEE)*, 2021, pp. 1–6.

[14] D. Slack, S. Krishna, H. Lakkaraju, and S. Singh, “Explaining machine learning models with interactive natural language conversations using TalkToModel,” *Nature Machine Intelligence*, vol. 5, no. 8, pp. 873–883, Aug. 2023, publisher: Nature Publishing Group. [Online]. Available: <https://www.nature.com/articles/s42256-023-00692-8>

[15] Q. Wang, T. Anikina, N. Feldhus, S. Ostermann, and S. Möller, “CoXQL: A dataset for parsing explanation requests in conversational XAI systems,” in *Findings of the Association for Computational Linguistics: EMNLP 2024*, Y. Al-Onaizan, M. Bansal, and Y.-N. Chen, Eds. Miami, Florida, USA: Association for Computational Linguistics, Nov. 2024, pp. 1410–1422. [Online]. Available: <https://aclanthology.org/2024.findings-emnlp.76/>

[16] L. Trigg, B. Morgan, A. Stringer, L. Schley, and D. F. Hougen, “Natural language explanation for autonomous navigation,” in *AIAA DATC/IEEE 43rd Digital Avionics Systems Conference (DASC)*, 2024.

[17] S. M. Lundberg and S.-I. Lee, “A unified approach to interpreting model predictions,” in *Proceedings of the 31st International Conference on Neural Information Processing Systems*, ser. NIPS’17. Red Hook, NY, USA: Curran Associates Inc., 2017, p. 4768–4777.

[18] M. Yildirim, B. Dagda, V. Asodia, and S. Falalah, “Highwayllm: Decision-making and navigation in highway driving with rl-informed language model,” *Robotics and Autonomous Systems*, vol. 193, p. 105114, 2025. [Online]. Available: <https://www.sciencedirect.com/science/article/pii/S0921889025002118>

[19] M. Ameur, B. Brik, and A. Ksentini, “Leveraging llms to explain drl decisions for transparent 6g network slicing,” in *2024 IEEE 10th International Conference on Network Softwarization (NetSoft)*, 2024.

[20] B. Mahbooba, M. Timilsina, R. Sahal, and M. Serrano, “Explainable Artificial Intelligence (XAI) to Enhance Trust Management in Intrusion Detection Systems Using Decision Tree Model,” *Complexity*, vol. 2021, no. 1, p. 6634811, 2021. [Online]. Available: <https://onlinelibrary.wiley.com/doi/abs/10.1155/2021/6634811>

[21] F. Aghaeipoor, M. Sabokrou, and A. Fernández, “Fuzzy rule-based explainer systems for deep neural networks: From local explainability to global understanding,” *IEEE Transactions on Fuzzy Systems*, vol. 31, no. 9, pp. 3069–3080, 2023.

[22] K. Hemker, Z. Shams, and M. Jamnik, “Cxplain: Rule-based deep neural network explanations using dual linear programs,” in *Trustworthy Machine Learning for Healthcare: First International Workshop, TML4H 2023, Virtual Event, May 4, 2023, Proceedings*. Berlin, Heidelberg: Springer-Verlag, 2023, p. 60–72. [Online]. Available: https://doi.org/10.1007/978-3-031-39539-0_6

[23] R. C. Engelhardt, M. Lange, L. Wiskott, and W. Koenen, “Sample-Based Rule Extraction for Explainable Reinforcement Learning,” in *Machine Learning, Optimization, and Data Science*, G. Nicosia, V. Ojha, E. La Malfa, G. La Malfa, P. Pardalos, G. Di Fatta, G. Giuffrida, and R. Umeton, Eds. Cham: Springer Nature Switzerland, 2023.

[24] V. Subhash, Z. Chen, M. Havasi, W. Pan, and F. Doshi-Velez, “What makes a good explanation?: A harmonized view of properties of explanations,” in *Progress and Challenges in Building Trustworthy Embodied AI*, 2022. [Online]. Available: <https://openreview.net/forum?id=YDyLZWwpBK2>

[25] K. Sokol and J. E. Vogt, “What does evaluation of explainable artificial intelligence actually tell us? a case for compositional and contextual validation of xai building blocks,” in *Extended Abstracts of the CHI Conference on Human Factors in Computing Systems*, ser. CHI EA ’24. New York, NY, USA: Association for Computing Machinery, 2024. [Online]. Available: <https://doi.org/10.1145/3613905.3651047>

[26] M. Matarese, F. Rea, K. J. Rohlfing, and A. Sciutti, “How informative is your XAI? Assessing the quality of explanations through information power,” *Frontiers in Computer Science*, vol. 6, p. 1412341, Jan. 2025. [Online]. Available: <https://www.frontiersin.org/articles/10.3389/fcomp.2024.1412341/full>

[27] L. Shi, Z. Tang, N. Zhang, X. Zhang, and Z. Yang, “A Survey on Employing Large Language Models for Text-to-SQL Tasks,” *ACM Comput. Surv.*, Jun. 2025, just Accepted. [Online]. Available: <https://dl.acm.org/doi/10.1145/3737873>

[28] Z. Juozapaitis, A. Koul, A. Fern, M. Erwig, and F. Doshi-Velez, “Explainable reinforcement learning via reward decomposition,” in *in proceedings at the International Joint Conference on Artificial Intelligence. A Workshop on Explainable Artificial Intelligence.*, 2019.

[29] DeepSeek-AI, “Deepseek-r1: Incentivizing reasoning capability in llms via reinforcement learning,” 2025. [Online]. Available: <https://arxiv.org/abs/2501.12948>